Electronic tattoos: the most multifunctional but imperceptible wearables

Jeong, Hyoyoung, Lu, Nanshu

Hyoyoung Jeong, Nanshu Lu, "Electronic tattoos: the most multifunctional but imperceptible wearables," Proc. SPIE 11020, Smart Biomedical and Physiological Sensor Technology XVI, 110200P (2 May 2019); doi: 10.1117/12.2518994

SPIE.

Event: SPIE Defense + Commercial Sensing, 2019, Baltimore, Maryland, United States

Electronic tattoos: the most multifunctional but imperceptible wearables

Hyoyoung Jeong[a], Nanshu Lu[b,*]
[a]Dept. of Electrical Engineering, University of Texas at Austin, Austin, TX USA 78712; [b]Center for Mechanics of Solids, Structures and Materials, Dept. of Aerospace Engineering and Engineering Mechanics, Dept. of Biomedical Engineering, Texas Materials Institute, University of Texas at Austin, Austin, TX USA 78712

ABSTRACT

Wearable electronics are finding emerging applications in mobile health, rehabilitation, prosthetics/exoskeletons, athletic training, human-machine interaction, etc. However, our skin is soft, curvilinear and dynamic whereas wafer-based electronics are hard, planar, and rigid. As a result, state-of-the-art wearables can only be strapped or clipped on human body. The development of flexible and stretchable electronics offers a remedy for such challenge. E-tattoos represent a class of stretchable circuits, sensors, and actuators that are ultrathin, ultrasoft, skin-conformable and deformable just like a temporary tattoo. We introduce a low-cost, dry and freeform "cut-and-paste" and "cut-solder-paste" method invented by my lab to fabricate e-tattoos. This method has been proved to work for thin film metals, polymers, ceramics, as well as 2D materials. Using these method, we created the first truly imperceptible e-tattoos based on graphene, and modular and reconfigurable Bluetooth and NFC enabled wireless e-tattoos.

Keywords: epidermal electronics, stretchable electronics, wearables, electronic tattoos, biometric sensors, wireless, digital manufacture

* Correspondence Email: nanshulu@utexas.edu; Phone: +1-512-471-4208

1. INTRODUCTION

Wearable electronics capable of long-term, ambulatory physiological monitoring could find many exciting applications in telemedicine, mobile health, prosthetics, athletic training, human-machine interface (HMI) and so on. However, the mechanical mismatch between wafer-based rigid electronics and the soft and curvilinear human body greatly hinders the wearability and functionality of state-of-the-art wearables. From "skin-like" electronics (e-skins) [1, 2] to "epidermal electronics" (e-tattoos) [3, 4], it is expected that the emerging technology of flexible/stretchable electronics will transform the wearable industry. For example, pressure-sensitive e-skins have been applied to measure pulse waves from the human wrist [5] and ultrathin photonic e-skins can be used as flexible oximeters when placed on the human fingertip [6]. Compared with e-skins which mostly refer to flexible electronics that can mimic human or animal skin functionalities, e-tattoos are ultrasoft, skin-conformable multifunctional membranes that can monitor a variety of biometrics including electrophysiological [7], thermal [8] and mechano-acoustic [9] signals, skin hydration [10], and even biomarkers in sweat [11]. However, after many years of research and development, it is still difficult to find soft wearable devices that are wireless, unobstructive, multimodal, yet affordable on the market. Among many remaining challenges, power supply and wireless data transmission are two outstanding ones. Near field communication (NFC) technology is known to be able to wirelessly transmit both power and data within centimeter range [12]. Recent publications demonstrated that it is possible to implement NFC into e-tattoos to make them go battery-free [13, 14]. NFC-enabled e-tattoos have found photometry [15-17] and radiometry [15, 18] applications. So far, however, NFC-enabled e-tattoos are not yet able to carry out electrophysiological (EP) or electrodermal activity (EDA) measurements. Moreover, although NFC circuits can be costly, they have to be disposed with the one-time use e-tattoo.

NFC enabled e-tattoos are currently fabricated by photolithography and transfer printing process [15, 16, 19], which can be expensive and time consuming. In 2015, our group invented a dry and desktop "cut-and-paste" process for the rapid prototyping of passive e-tattoos [20]. In this process, a mechanical cutter plotter can digitally carve out pre-designed

Smart Biomedical and Physiological Sensor Technology XVI, edited by Brian M. Cullum, Douglas Kiehl, Eric S. McLamore, Proc. of SPIE Vol. 11020, 110200P · © 2019
SPIE · CCC code: 0277-786X/19/$18 · doi: 10.1117/12.2518994

patterns on metal foils [20, 21], electrically conductive polymer sheets [20], or even 2D materials such as graphene [4, 22] within minutes. A slightly modified cut-and-paste method can even be used to pattern brittle ceramics such as indium tin oxide (ITO) into soft and stretchable ribbons [23]. After removing excessive regions, the leftover pattern can be transferred onto a target substrate such as a flexible medical tape or even human skin. The whole process takes only minutes and no cleanroom facilities or chemicals are required. Serpentine-shaped gold nanomembranes were patterned to be stretchable electrodes, resistance temperature detector (RTD), and hydration sensors. A double-stranded serpentine coil design was used to pattern aluminum micromembranes into a stretchable planar antenna [20]. The only limitation for the cut-and-paste process was the limited patterning resolution. We found that the ribbon width cannot go smaller than 200 μm [20].

To enable the integration of active electronic components on such e-tattoos, we here report a "cut-solder-paste" process. Within the context of the cutting method, the relatively low patterning resolution of the mechanical cutter plotter represents a major obstacle for building multifunctional wireless e-tattoos with reasonable footprint. To overcome such limitations, we herein propose a modular concept in which the NFC module, the functional circuitry, and the electrodes are first fabricated as separate layers and then stacked up as needed with vias aligned. The NFC and functional layers are reusable and can be disassembled and reassembled with other layers. Only the electrode layer needs to be disposed after each use. Such modular design allows for versatile combination of different layers to form wireless, battery-free e-tattoos capable of sensing a variety of biometrics including ECG & heart rate (HR), skin hydration, skin temperature, as well as pulse oximetry (SpO_2). The total size of the assembled e-tattoo is 7.4 cm x 5 cm, less than 190 μm thick (excluding chips), lighter than 1.3 grams, stretchable more than 30%, and has an effective modulus of 9.3 MPa. After 20 times disassembly and reassembly, the NFC and circuit layers remained fully functional. As a result, the modular NFC e-tattoo is a wear-and-forget wireless sensor system that is stretchable, unobstructive, and low cost. When scanned by an NFC-enabled smart-phone, the e-tattoo will harvest energy from the smart-phone, chips and LEDs on the e-tattoo will be powered by the harvested energy, and real-time data acquired by the e-tattoo will show up on a mobile app.

2. LOW-COST, DRY, AND FREEFORM MANUFACTURING FOR E-TATTOOS

The conventional cleanroom-based micro-fabrication method is not suitable for rapid prototyping or mass production of disposable medical patches such as epidermal electronics. We therefore invent a dry, benchtop, freeform and portable manufacturing method called the "cut-and-paste" and "cut-solder-paste" method to manufacture disposable epidermal sensor systems in a time and cost effective manner.

2.1 Conventional manufacturing process

Conventional manufacturing process of epidermal electronics relies on standard microelectronics fabrication processes. It involves vacuum deposition of thin films, spin coating, photolithography, wet or dry etching and transfer printing [3]. Although it has proven to be effective, there are several limitations associated with such processes. For example, this method depends on cleanroom-based facilities which are not portable, vacuum deposition and photolithography are time consuming, chemicals used in wet etching are hazardous to human body, wafers and masks used are expensive, and the rigid wafer is not compatible with roll-to-roll process. In this chapter, we report an innovative time- and cost-effective, benchtop, freeform, and portable fabrication method, which is applied to manufacture high-quality epidermal sensors. Detailed fabrication process of this new method is discussed and manufacture quality is investigated.

2.2 Cost and Time Effective "Cut-and-Paste" Method

A schematic of the "cut-and-paste" fabrication process is shown in Figure 1, snapshots of detailed experimental steps can be found in our paper [20]. The process starts with laminating a commercially available metal-coated PET foil (Goodfellow, USA) on a flexible, single-sided thermal release tape (TRT, Semiconductor Equipment Corp., USA) with the metal side touching the adhesive of the TRT. The other side of the TRT is then adhered to a tacky flexible cutting mat, as shown in Figure 1a. The cutting mat is fed into an electronic cutting machine (Silhouette Cameo, USA) with the PET side facing the cutting blade. By importing the AutoCAD design into the Silhouette Studio software, the cutting machine can automatically carve the Au-on-PET sheet with designed seams within minutes (Figure 1b). Once seams are formed, the TRT is gently peeled off from the cutting mat (Figure 1c). Slightly baking the TRT on a 115 °C hotplate for

1~2 minutes deactivates the adhesives on the TRT so that the excesses can be easily peeled off by tweezers (Figure 1d). The patterned devices are finally printed onto a target substrate with native adhesives, which could be a temporary tattoo paper (Silhouette) or a medical tape, such as 3M TegadermTM transparent dressing or 3M kind removal silicone tape (KRST) (Figure 1e), yielding an epidermal sensor system. Steps illustrated by Figure 1a to Figure 1e can be repeated for other thin sheets of metals and polymers, which can be printed on the same target substrate with alignment markers, rendering a multimaterial multifunctional system. For well-trained users, the entire process only takes about 15 minutes from beginning to end, which indicates that this new method has a significant advantage over conventional cleanroom-based fabrication approaches [20].

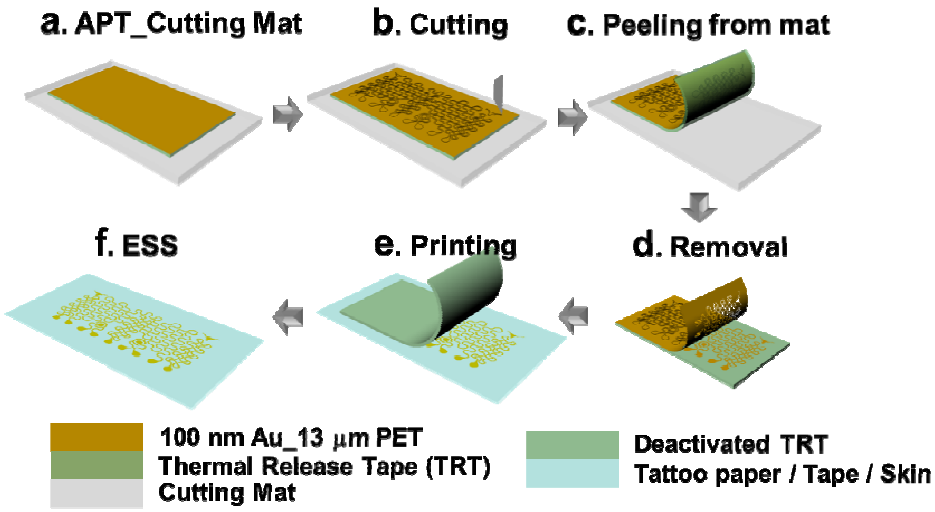

Figure 1. Schematics for the "cut-and-paste" process. (a) Au-PET-TRT (APT) laminated on the cutting mat with PET being the topmost layer. (b) Carving designed seams in the Au-PET layer by an automated mechanical cutting machine. (c) Peeling APT off the cutting mat. (d) Removing excessive Au-PET layer after deactivating the TRT on hot plate. (e) Printing patterned Au-PET layer onto target substrate. (f) Resulted epidermal sensor systems (ESS) with Au being the topmost layer [20].

2.3 "Cut-solder-paste" method for manufacturing wireless modular e-tattoos

A schematic of the "cut-solder-paste" method can be found illustrated in Figure 2, and is based on the "cut-and-paste" process detailed in our 2015 publication [20]. Both the generic NFC layer and the functional layers are fabricated utilizing the "cut-solder-paste" method, starting with laminating 18-μm-thick Cu foil (Copper 110 Annealed, ThyssenKrupp Materials) on a piece of TRT (Heat Release 3196, Semiconductor Equipment Corp) (Figure 2a). The TRT is adhered to a cutting mat, and pre-designed antennae and interconnects are engraved into the Cu foil using a mechanical cutter (Silhouette Cameo®, Silhouette America). The TRT and excess Cu foil are peeled from the mat, leaving the cut antenna and interconnect pattern, which is flipped and adhered to a water soluble tape (WST) (water-soluble wave solder tape 5414, 3M) laminated to a Kapton tape (DuPontTM), backed by a glass side (Figure 2b). Glass face side down, the construct is heated on a hot plate at 120°C for about 30 seconds and then cooled. The TRT is then peeled off, leaving the Cu pattern on the WST/Kapton Tape construct (figure 2c). Electrical components (NFC IC, AFE IC, photodetectors, LEDs, amplifiers, resistors, and capacitors) and interconnecting bridges are then soldered on the Cu circuit using conventional solder paste (Low Temp 138C, Chip Quik) according to the circuit designs. This is permissible due to the reasonably high thermal stability of the WST (240°C) and the Kapton tape (350°C). The glass slide is then kept on a hot plate at 220°C for the reflow purpose until soldering is complete (figure 2d). Once the components are fully soldered, the WST and circuitry are pasted onto Tegaderm tape (Figure 2e), and Kapton tape peeled off. The WST is dissolved with water droplets, leaving behind only the circuitry on the Tegaderm (Figure 2f) [24]. After the layers are fabricated, via holes are cut in the Tegaderm and double-sided z-axis conductive tapes are adhered to each via hole. Distinctive patterns at adjacent corners allow for the NFC layer to accurately stack onto the functional layer, and the stacked bilayer can laminate with the electrode layer. After training, it can take as little as one hour to construct a fully functional multilayer e-tattoo [25].

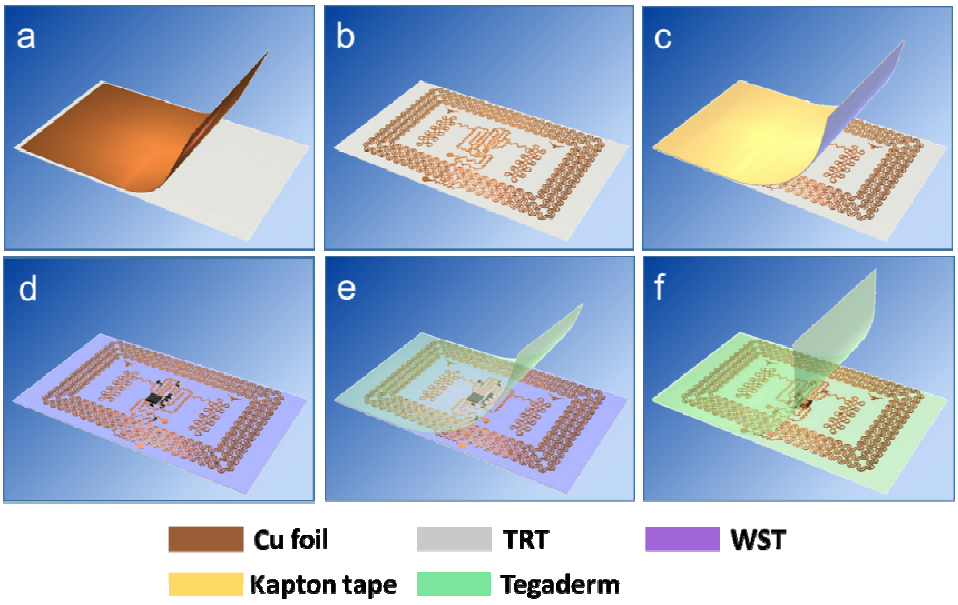

Figure 2. Schematics of the "cut-solder-paste" fabrication process for the modularized e-tattoo. (a) Copper foil is laminated on thermal release tape (TRT). (b) TRT is adhered to a cutting mat, and the pattern is carved into the Cu foil. TRT and access Cu is peeled from the mat. (c) The patterned Cu is transferred onto a water soluble tape (WST) supported by Kapton tape mounted on a glass slide by heating and removing the TRT. (d) ICs and other discrete components are soldered on the Cu. (e) The finished circuit is transferred to a Tegaderm tape, Kapton tape is removed, and WST is dissolved, resulting in a completed single layer e-tattoo. (f) The circuit may be sandwiched with another Tegaderm or stacked with multiple tattoo layers utilizing double-sided conductive tapes adhered via pads on different layers [24].

2.4 Graphene E-Tattoo Sensors (GETS)

The "wet transfer, dry patterning" fabrication process is illustrated in Figure 3. Detailed experimental steps can be found in our paper [4, 22]. "Wet transfer" refers to the copper etching step, which retains the high continuity of the large-area graphene grown on copper foil. "Dry patterning" refers to the use of a programmable mechanical cutter plotter to carve out the designed filamentary serpentine shapes on the graphene. Compared with photolithography, the dry patterning process minimizes the chemical contamination of graphene and is significantly more time- and cost-effective. Stepwise, graphene was first grown on a copper foil using atmospheric pressure chemical vapor deposition (APCVD) as previously reported (Figure 3a). As-grown CVD graphene on copper foil (Figure 3b) was characterized by scanning electron microscopy (SEM) and Raman spectroscopy. To retrieve the graphene from copper, sub-micrometer-thick poly(methyl methacrylate) (PMMA) was spin coated onto the as-grown graphene (Figure 3c), followed by copper etching (Figure 3d) and rinsing with deionized (DI) water. The graphene/PMMA (Gr/PMMA) bilayer was then transferred onto a piece of tattoo paper (Silhouette) with graphene facing up and PMMA in contact with the paper (Figure 3e). The sheet resistance of the Gr/PMMA was measured to be 1994.33 ± 264 Ω/□. Supported by the tattoo paper, the Gr/PMMA bilayer was carved into filamentary serpentine ribbons by a benchtop programmable mechanical cutter plotter (Silhouette Cameo) (Figure 3f). The serpentine ribbons were designed with a width of 0.9 mm and a radius of 2.7 mm to ensure the GET has a stretchability greater than that of skin. The extraneous areas of the Gr/PMMA were manually peeled off (Figure 3g), leaving a completed GET sensor on tattoo paper. The fabricated GET sensor can then be transferred onto any part of the glabrous or less-hairy skin, regardless of its curvature or shape, simply by bringing the graphene side in contact with the skin and wetting the backside of the tattoo paper to detach the GET from the paper (Figure 3h), exactly like a temporary transfer tattoo. No skin preparation or skin adhesive is required; the ultrathin GET can stay attached to the skin via just van der Waals interactions, as shown in Figure 3i [4, 22].

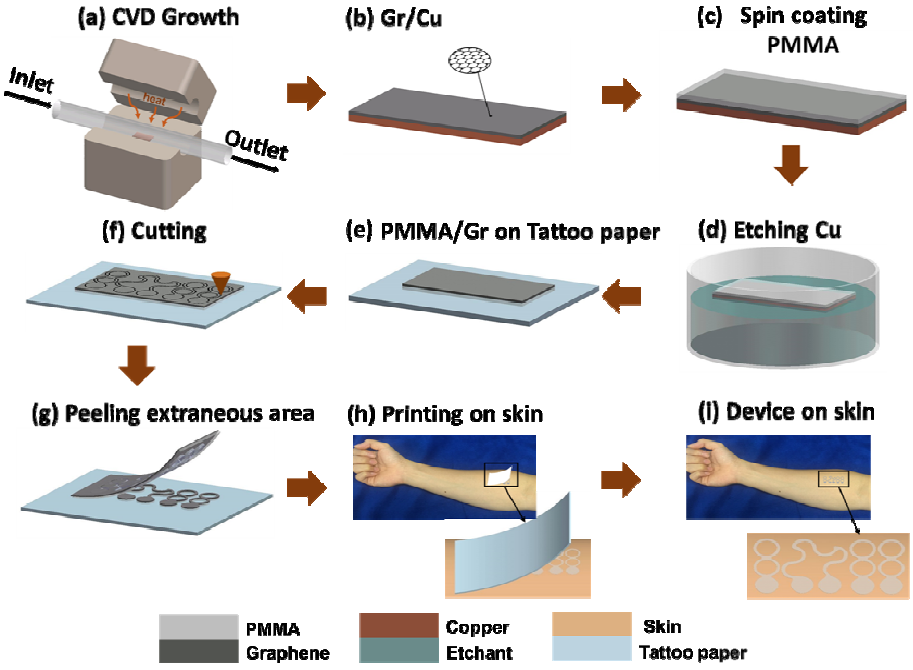

Figure 3. Fabrication process of GET. (a, b) Graphene was grown on copper foil using atmospheric pressure chemical vapor deposition system (APCVD). (c) Less than 500 nm thick PMMA was spin coated on graphene. (d) Copper was etched away. (e) Graphene/PMMA (Gr/PMMA) was transferred onto tattoo paper with PMMA touching the paper and graphene facing up. (f) Gr/PMMA was cut by a mechanical cutter plotter. (g) Extraneous Gr/PMMA was peeled off from the tattoo paper. (h) Mounting GET on skin like a temporary transfer tattoo. (i) GET on skin [4, 22].

3. MULTIFUNCTIONAL E-TATTOOS

Many health conditions of the human body can be reflected by non-invasive measurements of surface biosignals, such as surface ECG, surface EMG, surface EEG, skin temperature, skin hydration and respiratory rate. One of the main focuses in measuring surface biosignals is to capture high fidelity and low noise data in real time. Conventional measurement exploits rigid electrodes that are attached to human skin through wet gels, which may cause skin irritation or may dry out after long-term wearing. Emerging epidermal electronics exhibit low stiffness and high stretchability that are well matched with human skin. They are demonstrated to be compelling alternatives to conventional surface sensors. We developed a low-cost, bench-top manufacturing method for various stretchable e-tattoos. As a demonstration, this section will introduce a multimaterial, multifunctional e-tattoos, manufactured by these method. We demonstrated such e-tattoos to measure surface ECG, surface EMG, surface EEG, skin temperature, skin hydration and respiratory rate in a wired or wireless manner .

3.1 Cost Effective Epidermal Sensor System (ESS)

The top view of a multimaterial, multiparametric ESS supported by transparent temporary tattoo paper and its white liner is shown in Figure 4, which includes three Au-based filamentary serpentine (FS) electrophysiological (EP) electrodes which can be used for measurement of ECG, EMG and EEG, one Au-based FS resistance temperature detector (RTD), two Au-based dot-ring impedance sensors (for hydration measurement), and an Al/PET-based planar stretchable coil. In this picture, all Au-based sensors have the Au side facing up the stretchable coil, however, has the blue colored PET facing up because PET has demonstrated good biocompatibility but some people's skin can be allergic to Al. For the three EP electrodes, the inter-electrode distance is set to be 2 cm for effective EP signal recording. The FS is designed with a 1/5 ribbon width to arc radius ratio in order to balance the trade-off between stretchability and occupied area [20].

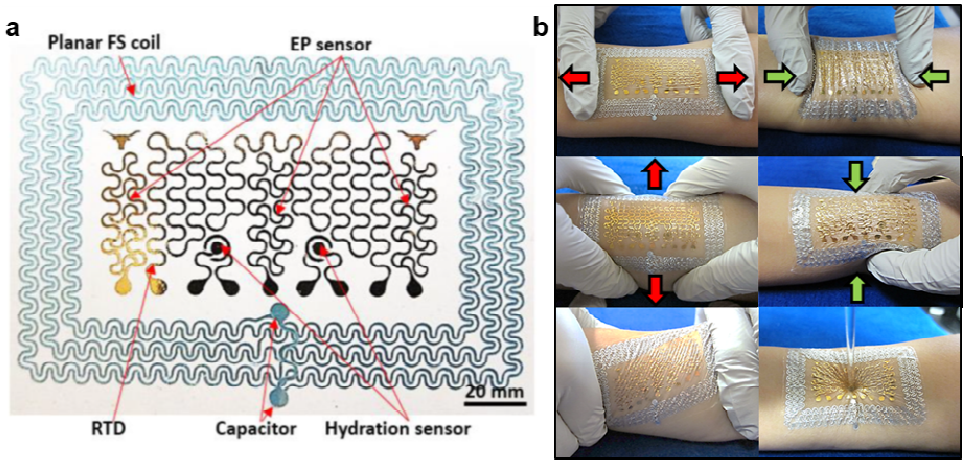

Figure 4. Epidermal Sensor System (ESS). (a) Top view of an ESS which incorporates three electrophysiological (EP) electrodes (Au-PET), a resistance temperature detector (RTD) (Au-PET), two coaxial dot-ring impedance sensors (Au-PET), and a wireless planar stretchable strain sensing coil (Al-PET), all in filamentary serpentine (FS) layout. (b) Deformability of ESS on human skin [20].

A deformability study was also conducted to evaluate the system-level mechanical response of the epidermal sensor system, as shown in Figure 4b. The patch has been subjected to different loading conditions such as stretching, compression, shear as well as surface rub and surface poking. Due to the small thickness and stretchable serpentine structure, the entire patch retains intimate contact with the skin under various loadings therefore exhibits high deformability [20].

Figure 5a shows ECG measured from human chest using silver/silver chloride (Ag/AgCl) gel electrodes and the ESS without applying any conductive gels. It is evident that the important features of ECG are captured by both electrodes,

but the ECG measured by our ESS demonstrates higher amplitude and more details compared with the Ag/AgCl electrodes. The intensity of the gripping force can be measured by a commercial dynamometer (Exacta™) and it is clear that the higher gripping force corresponds to higher signal amplitude in the measured EMG. Specifically, the average amplitude of the signal envelope corresponding to 44 N gripping force is about 3 times of that for a gripping force of 14 N (Figure 5b). The EEG has been measured by placing Ag/AgCl electrodes and the ESS on human forehead. Both electrodes are referenced against one FS electrode placed behind the human ear on the mastoid location, as shown in Figure 5c. The EEG measurements between conventional and ESS agree remarkably well and their FFT spectrums almost fully overlap in the upper right panel of Figure 5c, which confirms that conventional and ESS electrodes are almost indistinguishable in measured EEG signals [20].

Skin temperature measured by the epidermal RTD and the thermocouple are plotted in Figure 5d. The strong correlation between RTD and thermocouple outputs has validated the use of RTD as a compliant and stretchable skin temperature detector. Figure 5e illustrates a continuous hydration measurement with both epidermal hydration sensor and the corneometer before and after the subject drank a can of cold Espresso. The results are shown in Figure 5e, which clearly indicates gradual increase of hydration after drinking Espresso based on the measurements of both the epidermal hydration sensor and the corneometer. The test on skin was performed by applying Tegaderm-supported ECR-based strain gauges on the chest of a human subject and various respirational patterns have been studied. Figure 5f illustrates the deformation of human chest during normal breath and deep breath using the Wheatstone bridge. Larger amplitude and lower frequency are observed for deep breath [20].

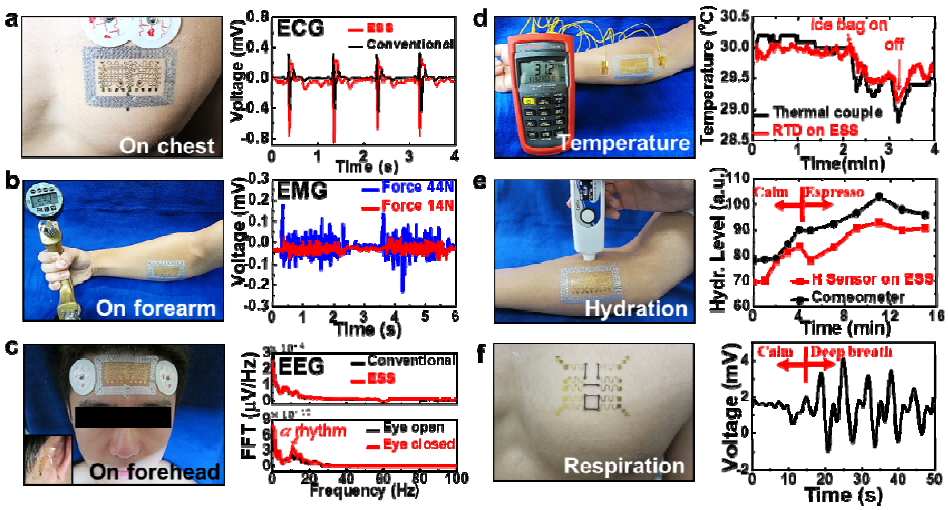

Figure 5. Biometrics measurement by Epidermal Sensor System. (a) ESS placed on human chest along with conventional Ag/AgCl electrodes to measure ECG. (b) ESS attached on human forearm for EMG measurement when the subject is gripping a commercial dynamometer with different forces. (c) EEG measured on human forehead by both ESS and Ag/AgCl electrodes. (d) Picture of RTD placed on the forearm along with traditional thermalcouple for temperature monitoring. (e) Picture of ESS placed on the forearm along with commercial coaxial corneometer for hydration monitoring. (f) Stretchable strain gauges made by electrically conductive rubber (ECR) on ESS for respiratory rate and pattern monitoring [20].

3.2 Modular and reconfigurable e-tattoos with wireless power and data communication

Near field communication (NFC) is a set of wireless communication protocols that allow devices to wirelessly transmit power and data when within close proximity to one another. Wireless e-tattoos have been fabricated utilizing this technology, but their manufacturing processes have included time and cost intensive photolithography and meticulous transfer printing. To more efficiently incorporate NFC into e-tattoos, we have proposed an extension of our previous process to a method coined “cut-solder-paste”. To take advantage of a cost-effective mechanical cutter, which has limited patterning resolution, we propose a modular concept (Figure 6a) that allows us to stack a generic NFC layer (Figure 6b),

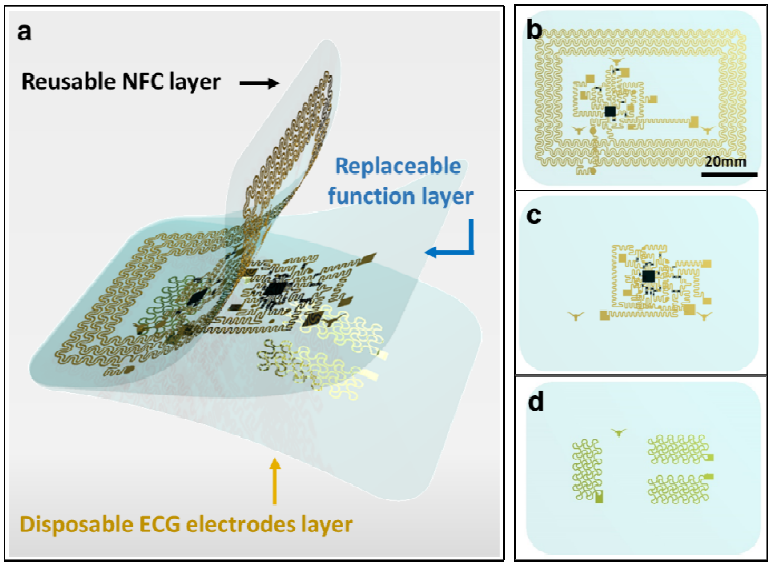

Figure 6. Schematic and photos of NFC-enabled, modular and reconfigurable e-tattoo. (a) Schematic of the e-tattoo, from top to bottom: NFC module, ECG circuit module, and electrode module. (b) Schematic of individual NFC layer. (c) Schematic of functional layer. (d) Schematic of electrode layer [25].

modular/replaceable functional layer(s) (Figure 6c), and an electrode layer (Figure 6d) aligned with vias. These multilayer e-tattoos are stretchable (up to 30%) and capable of wirelessly transmitting measured electrocardiogram (ECG), skin hydration, skin temperature, heart rate, and oxygen saturation (SpO_2).

We are able to demonstrate four different sensing modalities in our battery free, NFC enabled e-tattoos, including ECG, SpO_2, skin temperature and skin hydration. These can be measured in a single or dual mode operation, depending on the necessary application and design. Figures 7a-c showcase the single modality functionality with ECG data gathered from the e-tattoo placed at the lower ribcage at a 25 Hz sampling rate. Additionally, simultaneous measurement of two different sensing modalities is possible and shown in figures 7d. An NTC thermistor has been integrated into the NTC layer, and a skin hydration functional layer and an electrode layer were sequentially laminated onto the NFC layer. Approximately 5 minutes of skin conductance data was collected and compared with data simultaneously collected from a commercial corneometer (MoistureMeterSC Compact, Delfin Inc.). The e-tattoo data and reference data were overlaid, and show significant overlap (Figure 7e) [25].

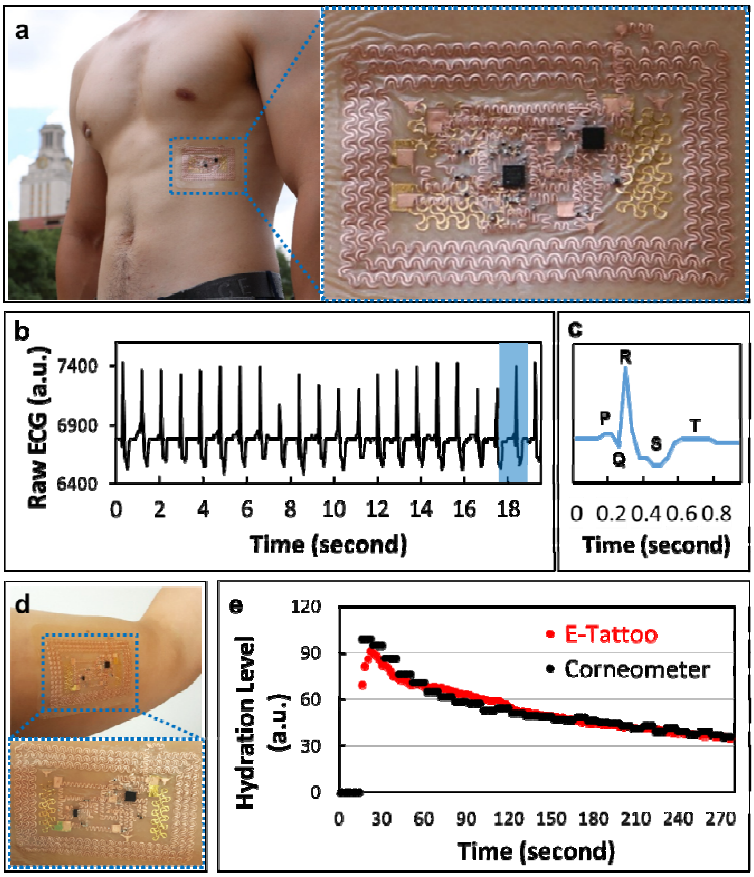

Figure 7. Multi-sensing modalities of the battery free, wireless e-tattoos. (a) The NFC-enabled e-tattoo applied at the lower rib cage of a male subject. (b) Raw ECG data as measured by the e-tattoo. (c) Magnified view of the ECG signal showcases the classic PQRST wave. (d) The hydration sensing e-tattoo on the upper arm of a subject. (e) Wirelessly measured skin hydration by the e-tattoo (red) and a commercial corneometer (black) before and after water application on the skin [25].

3.3 Transparent and Skin-Conformable GETS

A picture of an as-fabricated Gr/PMMA-based GET is shown in Figure 8a, in which different types of physiological sensors are labeled: graphene-based electrophysiological sensor (GEPS), resistance temperature detector (GRTD), and skin hydration sensor (GSHS). The GSHS shares one electrode with the GEPS. The total thickness of the GET was measured to be 463 ± 30 nm using a profilometer (Dektak 6 M Stylus). The average transmittance of PMMA and Gr/PMMA indicates that within the wavelength range of 400 to 800 nm the transmittance of bare PMMA is 96.5% to 98%, and the transmittance of GET is 84% to 88% due to additional light absorption by graphene [4, 22].

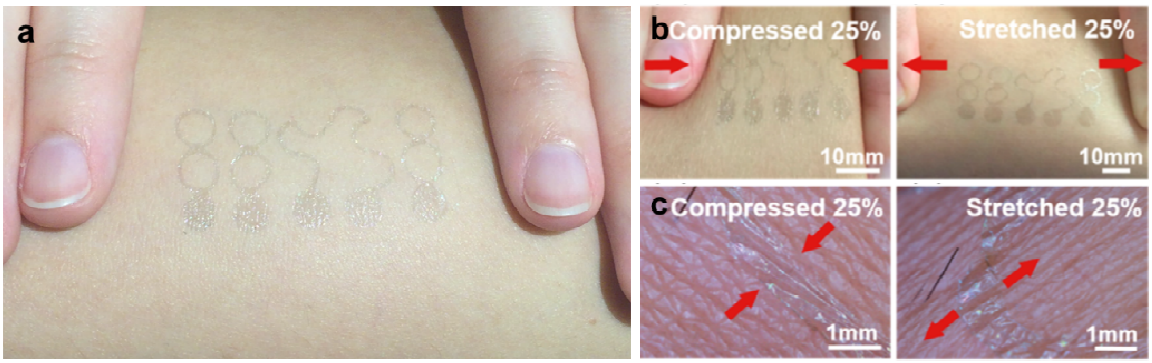

Figure 8. Picture of the as-fabricated GET. (a) GET mounted on skin. (b) GET on skin compressed and stretched by 25%, respectively. (c) Magnified photographs of a GET on compressed and stretched skin, which demonstrate its full conformability even under skin deformation [4, 22].

Figures 8b offers pictures of the GET on relaxed human skin and skin subjected to various kinds of deformations. Electrical resistance of the GEPS and GRTD was measured before and after arbitrary skin deformation, and no significant change could be identified. According to an analytical model we built previously, the GET has to be thinner than 510 nm to achieve full conformability with human skin. With our GET thickness being just 463 nm, optical micrographs of it on skin (Figures 8c) confirm the ultraintimate coupling between the GET and skin, even under severe skin deformation [4, 22].

Electrode−skin conformability directly dictates the contact impedance. Classical electrical circuit concepts suggest that the electrode−skin interface impedance is inversely proportional to the contact surface area. Since conformal contact increases the effective contact area, it is therefore expected that interface impedance decreases. We measured the GET−skin interface impedance and compared it with commercial Ag/AgCl gel−skin interface impedance, the latter of which is considered the gold standard for medical applications. The measurement was performed by laminating a GET on a human forearm without any skin preparation. The GSHS was connected to an LCR meter (Hioki 3532-50) using a customized flexible connector. A pair of Ag/AgCl gel electrodes were placed next to the GSHS with the same interelectrode distance, and the electrodes were connected to the LCR meter by alligator clips, as displayed in Figure 9a. The impedance was measured from 42 Hz to 2 kHz. The result shows that the GET−skin interface impedance is comparable with the gel electrode−skin impedance, although the GSHS surface area (~0.245 cm2) is more than 10 times smaller than that of the gel electrode (~2.6 cm2). Low contact impedance is essential for a high SNR in electrophysiological measurements.38 EEG, ECG, and EMG signals were measured using the GET (Figures 9b−f) and Gr/PI electrodes. The EEG signal was measured by laminating the GET on the forehead next to a commercial gel electrode, as shown in Figure 9b. No skin preparation was performed before mounting all the electrodes on the skin. It is evident in Figure 9b that the spectrograms of EEGs measured by the GET and gel electrodes are almost identical, and the blinks and alpha rhythms are clearly visible in both measurements. The GET can also be laminated on the human chest to measure an ECG. Figure 9c shows the measurement setup and the ECG signal recorded by an AvatarEEG through both a GEPS and commercial gel electrodes, with a 60 Hz digital notch filter applied. Characteristic ECG peaks (P, Q, R, S, T, and U) were clearly visible in both sets of data, but the GEPS measurement showed slightly higher signal magnitude. Application of a GET for EMG measurement was demonstrated by laminating a GET on the human forearm. The electrical activity of the forearm flexor muscle was measured using both the GEPS and commercial gel electrodes when the subject was squeezing a handgrip (Figure 9d). In addition to electrophysiological measurements, the GET is also able to measure skin temperature and hydration. Previous studies have demostrated that skin hydration level is monotonically correlated with skin impedance [4, 22].

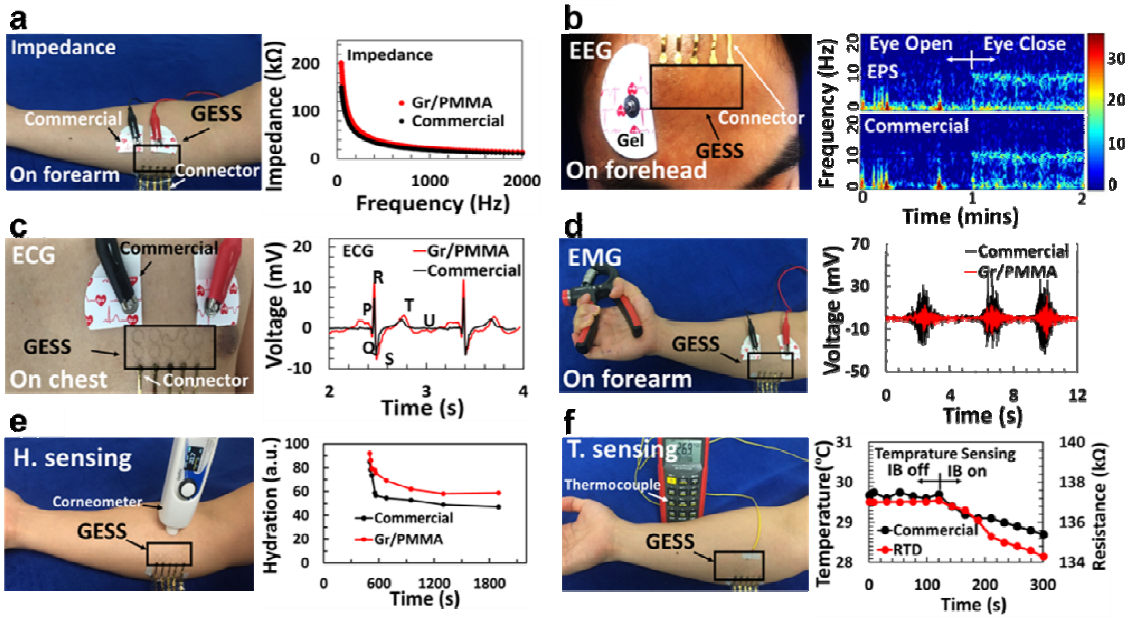

Figure 9. Electrical performance of the GET on skin. (a) Without any skin preparation, GET−skin contact impedance is almost on par with that between commercial gel electrodes and skin. (b) EEG sensing on the forehead with both the GET and gel electrodes (left). When the eyes were closed, an α rhythm of 10 Hz is visible in both spectrograms. (c) ECG measured synchronously by the GET and gel electrodes. Characteristic ECG peaks can be measured by both electrodes. (d) EMG sensing on the forearm with the GET and gel electrodes when the subject squeezed the hand exerciser three times. (e) Skin hydration sensing right after the application of body lotion, using both a GET and a commercial corneometer. (f) Skin temperature sensing with an ice bag placed in the vicinity of the GRTD and a thermocouple [4, 22].

4. CONCLUSIONS

E-tattoos, with their variability of conceptual applications and manufacturing methods, bring new value to epidermal electronics and personal biomedical wearables. Further research is necessary to truly take advantage of the capabilities of these devices in regards to types of biometrics that can be measured and signal distance, but integration with new state of the art wireless and analog front-end technologies will greatly expand its applications. The tattoo-like application form factor offered by these devices will play a significant role in shaping the future of mobile healthcare, as they offer a more unobstructive, affordable, and reliable sensing modality when compared to the current unimodal offerings. Additionally, we predict that the integration of NFC into current e-tattoo will allow them to become more prevalent in the IoT industry as an alternative biometric sensing solution.

ACKNOWLEDGEMENTS

This work is based upon work supported in part by US National Science Foundation (NSF) Division of Electrical, Communications and Cyber Systems (ECCS) under Grant no. 1509767. The biometric sensor development and human subject validation was supported by US Office of Naval Research (ONR) under Grant no. N00014-16-1-2044. Any opinions, findings and conclusions or recommendations expressed in this material are those of the authors and do not necessarily reflect the views of the National Science Foundation nor Office of Naval Research.

REFERENCES

[1] T. Someya, T. Sekitani, S. Iba *et al.*, "A large-area, flexible pressure sensor matrix with organic field-effect transistors for artificial skin applications," Proceedings of the National Academy of Sciences, 101(27), 9966-9970 (2004).

[2] M. L. Hammock, A. Chortos, B. C. K. Tee *et al.*, "25th anniversary article: the evolution of electronic skin (e□skin): a brief history, design considerations, and recent progress," Advanced materials, 25(42), 5997-6038 (2013).

[3] D.-H. Kim, N. Lu, R. Ma *et al.*, "Epidermal electronics," science, 333(6044), 838-843 (2011).

[4] S. Kabiri Ameri, R. Ho, H. Jang *et al.*, "Graphene electronic tattoo sensors," ACS nano, 11(8), 7634-7641 (2017).

[5] G. Schwartz, B. C.-K. Tee, J. Mei *et al.*, "Flexible polymer transistors with high pressure sensitivity for application in electronic skin and health monitoring," Nature Communications, 4(1), 1859 (2013).

[6] T. Yokota, P. Zalar, M. Kaltenbrunner *et al.*, "Ultraflexible organic photonic skin," Science Advances, 2(4), e1501856-e1501856 (2016).

[7] J.-W. Jeong, W.-H. Yeo, A. Akhtar *et al.*, "Materials and Optimized Designs for Human-Machine Interfaces Via Epidermal Electronics," Advanced Materials, 25(47), 6839-6846 (2013).

[8] R. C. Webb, A. P. Bonifas, A. Behnaz *et al.*, "Ultrathin conformal devices for precise and continuous thermal characterization of human skin," Nature Materials, 12(10), 938-944 (2013).

[9] Y. Liu, J. J. Norton, R. Qazi *et al.*, "Epidermal mechano-acoustic sensing electronics for cardiovascular diagnostics and human-machine interfaces," Sci Adv, 2(11), e1601185 (2016).

[10] X. Huang, H. Cheng, K. Chen *et al.*, "Epidermal Impedance Sensing Sheets for Precision Hydration Assessment and Spatial Mapping," IEEE Transactions on Biomedical Engineering, 60(10), 2848-2857 (2013).

[11] H. Lee, T. K. Choi, Y. B. Lee *et al.*, "A graphene-based electrochemical device with thermoresponsive microneedles for diabetes monitoring and therapy," Nature Nanotechnology, 11(6), 566 (2016).

[12] K. Finkenzeller, [RFID handbook: fundamentals and applications in contactless smart cards, radio frequency identification and near-field communication] Wiley-Blackwell, Oxford(2010).

[13] J. Kim, A. Banks, H. Y. Cheng *et al.*, "Epidermal Electronics with Advanced Capabilities in Near-Field Communication," Small, 11(8), 906-912 (2015).

[14] J. Kim, A. Banks, Z. Xie *et al.*, "Miniaturized Flexible Electronic Systems with Wireless Power and Near-Field Communication Capabilities," Advanced Functional Materials, 25(30), 4761-4767 (2015).

[15] J. Kim, G. A. Salvatore, H. Araki *et al.*, "Battery-free, stretchable optoelectronic systems for wireless optical characterization of the skin," Science Advances, 2(8), e1600418-e1600418 (2016).

[16] J. Kim, P. Gutruf, A. M. Chiarelli *et al.*, "Miniaturized Battery-Free Wireless Systems for Wearable Pulse Oximetry," Advanced Functional Materials, 27(1), 1604373 (2017).

[17] G. Shin, A. M. Gomez, R. Al-Hasani *et al.*, "Flexible Near-Field Wireless Optoelectronics as Subdermal Implants for Broad Applications in Optogenetics," Neuron, 93(3), 509-521.e3 (2017).

[18] H. Araki, J. Kim, S. Zhang *et al.*, "Materials and Device Designs for an Epidermal UV Colorimetric Dosimeter with Near Field Communication Capabilities," Advanced Functional Materials, 27(2), 1604465 (2017).

[19] S. Han, J. Kim, S. M. Won *et al.*, "Battery-free, wireless sensors for full-body pressure and temperature mapping," Science Translational Medicine, 10(435), eaan4950 (2018).

[20] S. Yang, Y.-C. Chen, L. Nicolini *et al.*, ""Cut-and-Paste" Manufacture of Multiparametric Epidermal Sensor Systems," Advanced Materials, 27(41), 6423-6430 (2015).

[21] Y. Wang, Y. Qiu, S. K. Ameri *et al.*, "Low-cost, μm-thick, tape-free electronic tattoo sensors with minimized motion and sweat artifacts," npj Flexible Electronics, 2(1), (2018).

[22] S. K. Ameri, M. Kim, I. A. Kuang *et al.*, "Imperceptible electrooculography graphene sensor system for human–robot interface," npj 2D Materials and Applications, 2(1), (2018).

[23] S. X. Yang, E. Ng, and N. S. Lu, "Indium Tin Oxide (ITO) serpentine ribbons on soft substrates stretched beyond 100%," Extreme Mechanics Letters, 2, 37-45 (2015).

[24] H. Jeong, T. Ha, I. Kuang *et al.*, "NFC-enabled, tattoo-like stretchable biosensor manufactured by "cut-and-paste" method." 4094-4097.

[25] H. Jeong, L. Wang, T. Ha *et al.*, " Modular and Reconfigurable Stretchable Electronic Tattoos for Personalized Sensing," Advanced Materials Technologies, DOI: 10.1002/admt.201900117, (2019).